CANCON2026 Proceedings: Exploring the Hidden Influence of Crack Parallel Tension on Interlaminar Fracture Toughness in Quasibrittle Composites

Genki Matsubara, Marco Salviato

April 2026

Abstract

Recent research challenges the traditional Linear Elastic Fracture Mechanics (LEFM) assumption that crack parallel stresses have minimal impact on fracture toughness. Gap test results reveal that in quasibrittle materials, Mode I fracture energy is significantly affected by crack parallel compression. While compressive stress increases fracture energy up to a point, it eventually leads to a reduction near the material's compressive strength. In carbon fiber laminates, intra-laminar fracture energy decreases steadily under parallel compression. The Crack Band Model (CBM) effectively captures this behavior, unlike Cohesive Zone Models (CZMs), which fell short to represent the finite-thickness Fracture Process Zone (FPZ). Building on this, we introduce the Half Open-I test, a novel method to assess Mode I interlaminar fracture energy under crack parallel tensile stress. The test uses localized moments at the crack opening to evaluate fracture energy, revealing how tensile stress affects FPZ size and total fracture energy. This new approach corrects previous over/under-estimations in fracture toughness and offers more accurate predictions for the integrity of quasibrittle composite structures.

Keywords: Composite, Quasibrittle Fracture Mechanics, Crack Parallel Stress.

Corresponding author: Genki Matsubara

1 Introduction

The application of composite materials to aircraft structures has increased markedly in recent years, accompanied by greater diversity in the materials employed [1–5]. Consequently, there is an increasing need for new design and safety evaluation methodologies that account for the distinctive fracture behavior of composite materials, which differs substantially from that of conventional metallic structures. Among the advanced materials adopted in aerospace applications, carbon fiber reinforced polymers have experienced particularly widespread growth [6].

Conventional metallic materials such as aluminum alloys generally exhibit noticeable plastic deformation prior to failure. In contrast, composite materials show fundamentally different damage and fracture mechanisms, including interlaminar delamination and other progressive failure modes [7–16]. Consequently, alongside traditional strength-based design approaches, fracture mechanics-based methods for evaluating crack initiation and propagation have become increasingly important. Linear Elastic Fracture Mechanics (LEFM) provides the basic theoretical framework for fracture analysis; however, many engineering materials exhibit nonlinear behavior near the crack tip. Dugdale addressed this nonlinearity primarily through plastic yielding in metals, whereas Barenblatt introduced the concept of a softening region ahead of the crack tip, later referred to as the Fracture Process Zone (FPZ) [14, 17]. Traditionally, LEFM assumes that the total fracture energy, G_F, is unaffected by crack parallel stress. However, the gap test proposed by Nguyen and Bažant et. al. [18] demonstrated that G_F initially increases under crack parallel compressive stress and subsequently decreases at higher compression levels. This behavior was attributed to friction-induced enlargement of the FPZ, which was successfully reproduced using the Microplane Model M7 [18, 19]. Brockmann and Marco Salviato later extended the gap test concept to composite laminates [5]and showed that crack parallel stress significantly influences G_F in ways that conventional CZM formulations fail to capture.

The foregoing findings demonstrate that crack parallel stress can substantially influence the fracture behavior of materials, and its effects cannot be neglected in either experimental or numerical investigations. In practical engineering applications, structural components are frequently subjected to complex multiaxial stress states rather than the simplified uniaxial loading conditions commonly assumed in laboratory testing [18–21]. As a result, concerns have emerged that the structural strength of many systems may have been overestimated due to the omission of crack parallel stress effects in design and assessment methodologies.

This issue is of particular importance for large-scale engineering structures, including aircraft, buildings, automobiles, wind turbines, railway vehicles, ships, power plants, jet engines, combustion turbines, and nuclear reactors. Even in cases where no visible fracture exists immediately after manufacturing or construction, fatigue damage and crack growth influenced by crack parallel stress may lead to premature structural failure before the intended service life is reached.Accordingly, fracture behavior under crack parallel stress states has become an important research topic for both structural safety assessment and the development of lightweight engineering systems. Nevertheless, many fundamental aspects of these effects remain insufficiently understood.

Since the original introduction of the gap test, investigations into fracture behavior under crack parallel stress have focused predominantly on compressive loading conditions [5, 18, 19, 21]. This emphasis is reasonable for infrastructure materials such as concrete, in which crack propagation under compression commonly occurs in service environments. In contrast, carbon fiber reinforced polymers, which are extensively employed in aerospace structures, are required to retain damage tolerance even under severe tensile loading conditions [22, 23]. The original gap test study also suggested that the methodology could potentially be extended to crack parallel tensile stress states [18].However, such an extension would require the development of new loading fixtures and experimental configurations. Moreover, compared with the polypropylene pad system used to generate relatively uniform crack parallel compression, tension-based gap test configurations may present greater challenges especially for the advanced composites in terms of material strength. Furthermore, the need to generate localized stress through pad contact introduces a risk of transverse fracture [24, 25]. In addition, the application of the gap test under crack parallel tension conditions requires the introduction of fixture designs and the use of high-strength loading pads. Given the high material cost of composites and the complexity of the testing procedure, there is a pressing need for the development of a practical and reliable test method tailored for this purpose.

2 Methods

2.1 Half Open-I Test: Interlaminar Fracture Test With Crack Parallel Tension

In this study, a novel and simplified experimental configuration, referred to as the Half Open-I (HOI) test, is proposed to investigate the effects of crack parallel tensile stress on the fracture energy G_F and FPZ development during interlaminar crack propagation in carbon fiber composites. A distinguishing characteristic of the proposed method is that both the Mode I opening stress and the crack parallel tensile stress are generated simultaneously through local bending moments arising from the specimen geometry, even under externally applied uniaxial loading conditions. (Figure 1). As a result, the HOI configuration provides a significantly simpler approach for introducing crack parallel tensile stress. In the proposed geometry, the magnitude of the local bending moment, and consequently the crack parallel tensile stress near the crack tip, can be controlled by inserting tabs with different thicknesses at the crack-mouth of the specimen. This enables systematic tuning of the local stress state while preserving the simplicity and practicality of uniaxial testing. Furthermore, owing to the absence of complex loading fixtures and the geometrical simplicity of the specimen, the proposed method offers a cost-effective means of evaluating G_F under crack parallel tensile loading conditions.

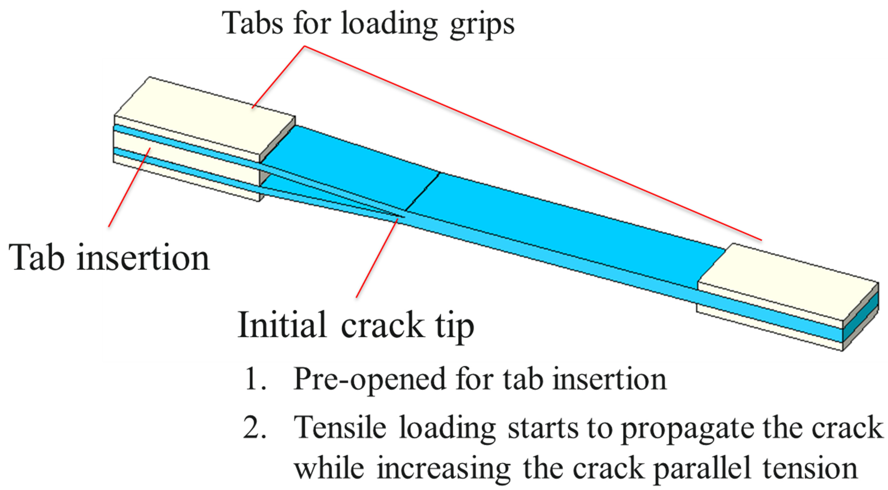

Figure 1: Half Open-I test geometry

2.2 Features and Strategy for R-curve

The present study emphasizes two essential features of the HOI geometry: (i) the configuration behaves as a negative geometry, and (ii) the crack parallel stress state changes continuously during crack propagation.

In many conventional fracture test configurations, the energy release rate (SERR) increases as the crack extends, and such configurations are generally categorized as positive geometries. In contrast, geometries in which the SERR decreases with increasing crack length are classified as negative geometries [17]. Positive geometries commonly exhibit a distinct peak load during testing, occurring when the SERR curve becomes tangent to the R-curve with the same slope. Under this condition, the G_F and the FPZ length c_f can be evaluated directly using size-effect approaches such as Bažant's Type II Size Effect Law (BSL) [17]. In practical engineering structures subjected to load-controlled conditions, crack growth beyond this critical state becomes unstable and typically results in catastrophic failure. Accordingly, the peak load is generally regarded as the governing parameter that defines structural strength. In contrast, negative geometries exhibit a decreasing SERR as crack propagation progresses, and therefore fracture mechanics does not predict the existence of a distinct upper limit for structural strength i.e. the peak load. More specifically, under constant loading conditions, the SERR curve does not become tangent to the R-curve with an identical slope. A major limitation of such geometries is the absence of a clearly defined peak load, which prevents the direct application of BSL for evaluating the G_F and c_f.

The second characteristic of the HOI geometry is that the specimen is subjected to uniaxial loading, under which both the crack parallel tensile stress and the local bending moment responsible for Mode I crack opening increase simultaneously with the applied axial load. Consequently, crack propagation and crack parallel stress evolve concurrently during the experiment, suggesting that the resulting R-curves may vary depending on the specific test geometry. To address this issue, the present study proposes conducting multiple HOI tests using different inserted tab thicknesses. The thickness of the tabs placed at the specimen end can be selected arbitrarily, provided that excessive loading leading to premature crack propagation is avoided. By adjusting the tab thickness, the bending moment generated under axial loading can be systematically controlled, thereby regulating the crack parallel tensile stress acting during crack extension. A series of experiments performed with different tab thicknesses enables the construction of R-curves corresponding to fixed tab configurations. Although the shapes of these R-curves may differ depending on the tab geometry, the intrinsic material behavior itself should remain unchanged. Accordingly, this approach allows the influence of crack parallel tensile stress on fracture behavior to be evaluated in a systematic and objective manner.

2.3 Material, Specimen Design and Fabrication

The material system investigated in this study was IM7/977-3, consisting of IM7 carbon fibers embedded within a 977-3 thermosetting epoxy matrix [26]. IM7 is a high-strength, intermediate-modulus PAN-based continuous carbon fiber, whereas 977-3 is an epoxy resin designed for autoclave and press-cure processing applications. [27]. The fundamental mechanical properties of this system have been reported by Clay et al. [26].

Owing to the strong biaxial stress concentration generated near the crack tip in this geometry, there exists a possibility of premature fiber splitting occurring before stable crack propagation can be achieved. To reduce this risk, a cross-ply laminate with the stacking sequence $[0/90/0/90/0]_s$ was employed. The specimen dimensions were 270 mm $\times$ 25 mm $\times$ 1.3 mm, corresponding to a nominal ply thickness of 0.13 mm (Figure 2(a)). Tabs with a length of 45 ± 5 mm were were adhesively bonded to both ends of the specimen. An initial crack length of 50 mm was introduced, providing a gauge section length of 170 mm . This configuration was selected to minimize unintended crack extension during tab insertion and gripping in the testing apparatus (Figure 2(b)).

The IM7/977-3 laminate specimens used in this study were manufactured according to the following procedure. Rolls of uncured IM7/977-3 prepreg were stored under refrigerated conditions and allowed to equilibrate at room temperature. The prepreg sheets were subsequently cut into rectangular plies using a Zünd G3 L-2500 digital cutting system at the University of Washington Advanced Composites Center [28]. The cut plies were hand-laid on a steel tooling plate according to the specified stacking sequence. To introduce an artificial interlaminar crack, a 0.0005-inch (approximately 12.7 μm) Teflon film (DuPont™ Type A Optically Clear FEP Film made with Teflon™ fluoroplastic) was inserted at the mid-plane during layup. During the layup process, vacuum debulking was performed every five plies for approximately 10 min in order to enhance laminate consolidation. The FEP insert was positioned at the laminate mid-plane to introduce the initial delamination crack. After completing the layup, a final vacuum debulking step lasting 7–12 hours was carried out to reduce interlaminar void formation. After completion of the layup process, the laminate was vacuum bagged using a conventional sandwich arrangement consisting of vacuum bagging film (Wrightlon® WL7400), release film (A4000), and breather fabric (Airweave® N10). To further reduce interlaminar porosity, an extended vacuum debulking stage lasting approximately 7–12, h was carried out prior to curing. The laminate was subsequently cured in an autoclave produced by American Autoclave following the manufacturer-recommended cure schedule. The cure cycle involved a gradual temperature ramp to approximately 350°F, followed by a dwell period and subsequent cooling.

Following curing, Garolite G-10 fiberglass tabs were adhesively bonded to the laminate using a two-part epoxy adhesive manufactured by J-B Weld to provide gripping surfaces during testing. Test specimens were subsequently cut from the laminate using an MK 101 wet tile saw produced by MK Diamond. The wet-cutting process was adopted to limit thermal buildup and reduce machining-induced fiber damage. Prior to testing, a pre-crack was introduced in accordance with the ASTM standard for Double Cantilever Beam (DCB) test [29]. A representative specimen configuration is presented in Figure 2(a).

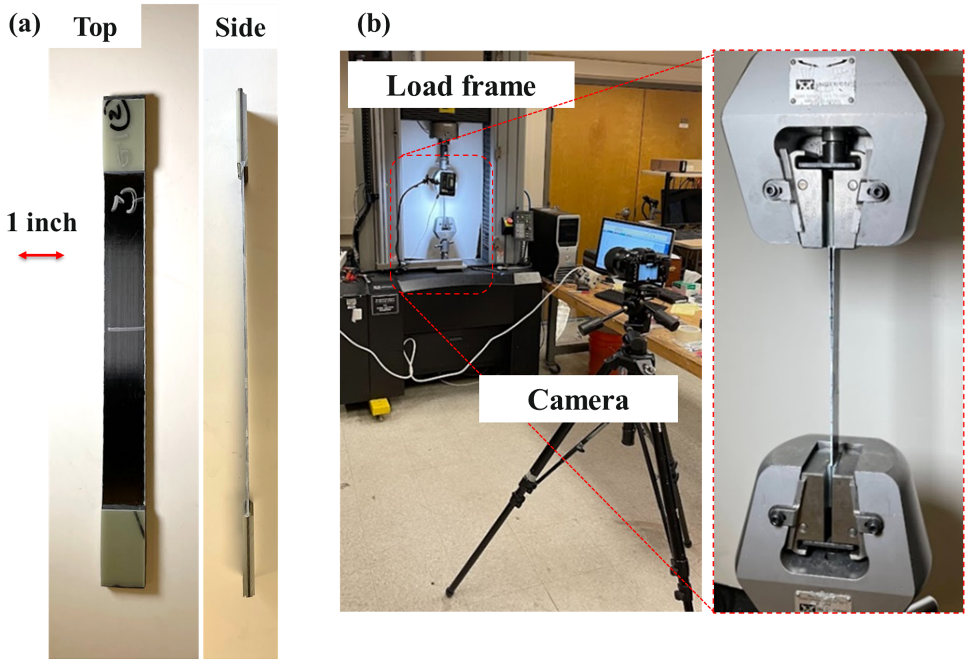

Figure 2: Test Configuration. (a) Half Open-I specimen geometry prior to testing (b) Overview of the Half Open-I test configuration in the Instron 5585H load frame

3 Results

3.1 R-curve

The load–displacement responses obtained from the HOI specimens are presented in Figure 4. The apparent stress at final failure is notably lower than the reported tensile strength of unidirectional IM7/977-3 laminates [26]. This behavior can be attributed to the combined stress state arising from the superposition of the applied axial stress and the additional stress generated by bending moments induced by the inserted tab thickness.

For the evaluation of the R-curve, crack length measurements were obtained directly from recorded digital images [17, 23]. To improve visibility of the crack tip during testing, the specimen surfaces were coated with white paint prior to loading. Digital images were captured at a frequency of one frame per second throughout the tensile tests, which were conducted using an Instron 5585H universal testing machine (Figure 2(b)). The crack-tip progression observed during testing is presented in Figure 3. No measurable crack growth occurred during the clamping stage. With increasing applied tensile load, crack initiation was followed by stable propagation until catastrophic failure associated with fiber fracture occurred. Unlike the load–displacement response commonly observed in positive geometries, the present configuration exhibited no pronounced load drop prior to final failure, except for the sudden decrease in load corresponding to fiber rupture.

Although size-effect-based methods generally provide a more robust approach for determining R-curves, such techniques are limited to positive geometries and therefore cannot be directly applied to the present HOI geometry. Thus, R-curve evaluation was attempted from the load–displacement data with the directly determined crack length using compliance-based methods or fracture energy–area approaches [17, 23]. However, these methods rely on a measurable reduction in stiffness caused by crack propagation. Although such approaches are, in principle, applicable to the present results, the load reduction associated with crack growth is too subtle to be reliably quantified, while the measured displacement contains significant experimental uncertainty. Consequently, alternative methods are required, such as finite element analysis or analytical formulations that directly relate the applied load to the SERR for a given crack length. So, R-curves here are evaluated using the J-integral by Abaqus/Standard 2023 for nonlinear deformations.

The resulting R-curve obtained from the 2.4 mm tab configuration is shown in Figure 5(a). The curve

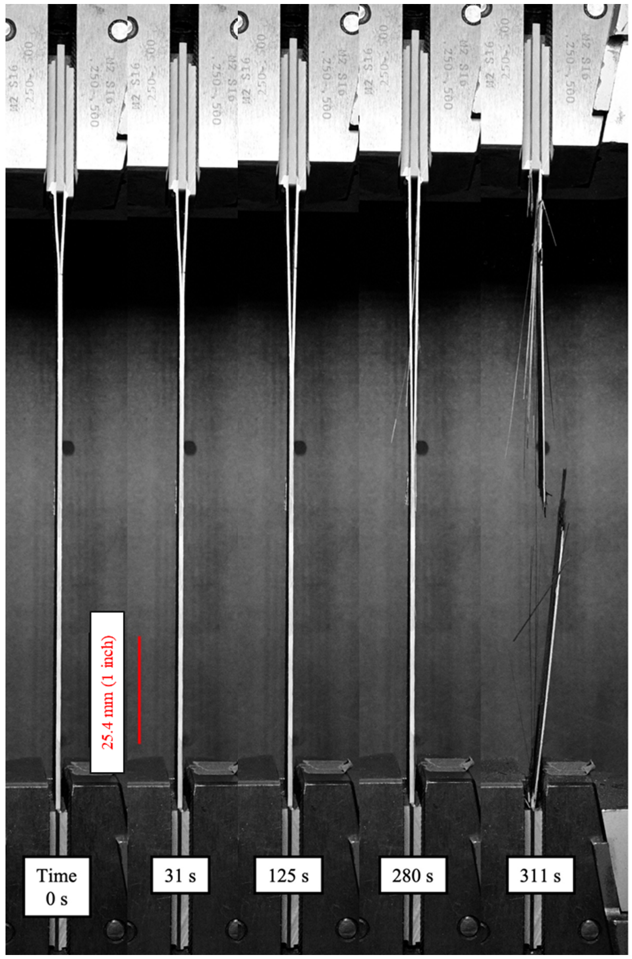

Figure 3: Crack propagation observed during the HOI test with an inserted tab thickness of 2.4mm.

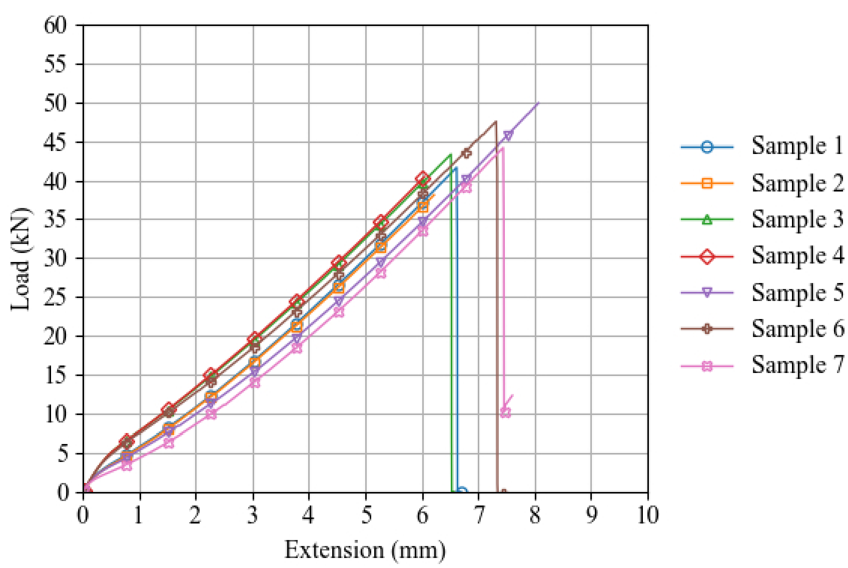

Figure 4: Load–displacement curves of the HOI test with 2.4mm tab inserted. The tests were executed till fiber failure or 50 kN.

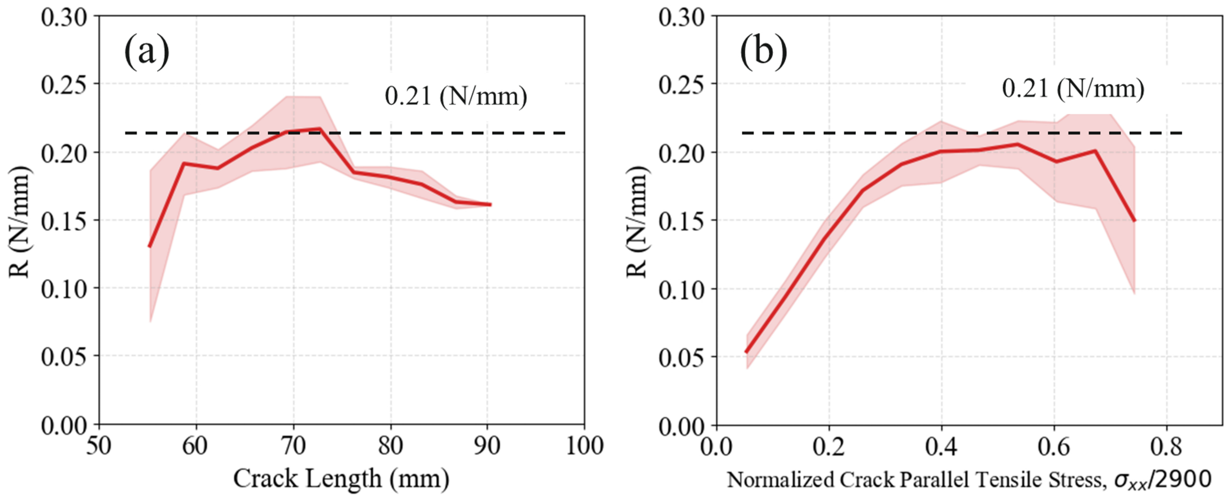

Figure 5: (a) R-curve the HOI test with 2.4mm thick tab inserted (b) Crack propagation resistance to the normalized crack parallel tensile stress (Shaded for 1 σ, the dashed line stands for the typical reported G_F)

displays a rising trend up to a crack length of approximately 70mm, suggesting comparable FPZ development during the early stages of crack propagation. Beyond this crack length, however, a significant decrease in the R-curve is observed. Under the assumptions of LEFM or an idealized line-crack representation, G_F is expected to remain independent of crack parallel stress, and the R-curve should approach a plateau once a self-similar FPZ and steady-state crack growth are established [14, 17]. In contrast, the HOI test results demonstrate a clear reduction to values below the representative literature value of 0.21N/mm [26, 27, 30–32], while the R-curve decreases rather than converging to a stable plateau as the crack parallel tensile stress increases. These findings are inconsistent with the fundamental assumptions of the line-crack model. The crack growth resistance is also plotted against crack parallel tensile stress in Figure 5(b). Here, the crack parallel tensile stress refers to the local longitudinal stress acting in the unidirectional (UD) ply at the uncracked end of the specimen, the ply bridging the crack-tip region. The crack growth resistance initially increases with increasing crack parallel tensile stress up to approximately 40% of the UD tensile strength, where the UD tensile strength is 2900 MPa [26]. The gradual rise in R-curve before significant crack propagation suggests that the FPZ continues to evolve during this stage. However, once the crack parallel tensile stress exceeds approximately 50% of strength, the resistance begins to decline. This behavior is fully consistent with the trends observed in the previously presented R-curves. Notably, prior to this transition, the FPZ development appears essentially identical to and the plateau resistance values closely correspond to the representative interlaminar fracture energy reported in the literature.

Beyond approximately 50% of the UD tensile strength, the assumptions inherent to LEFM and idealized line-crack models are no longer adequate to describe the observed behavior. Instead, quasibrittle effects become increasingly dominant, resulting in a progressive reduction in crack growth resistance with increasing crack parallel tensile stress. This suggests that the observed degradation in resistance is governed directly by the crack parallel tensile stress itself, rather than by crack propagation rate or other time-dependent effects.

3.2 SEM Fractographic Analysis

Fractographic analysis of the fracture surfaces was conducted by the scanning electron microscopy (SEM). The imaging was conducted at the University of Washington Molecular Analysis Facility (MAF) [33], and the instrument used was the ThermoFisher Apreo-S [34], a high-resolution scanning electron microscope capable of single-nanometer spatial resolution. Representative SEM results are shown in Figure 6. In region (a), corresponding to the area near the initial crack tip where no visible whitening is observed at the macroscopic scale, the matrix resin exhibits sharp, brittle fracture at the microscopic level. Within the observed field, significant fiber–matrix debonding or resin pull-out from fibers was not evident. In contrast, in region (b), corresponding to the macroscopically whitened area, the matrix resin appears fragmented into fine, fibrillated features. Moreover, clear exposure of carbon fibers is observed due to matrix detachment from the fiber surface. This indicates a transition in fracture mechanism.

In the HOI configuration, crack propagation in the early stage occurs under conditions where crack parallel stress is minimal. Mechanically, this stage is therefore close to conventional Mode I interlaminar fracture, such as in a DCB specimen where crack parallel stress is negligible. In the later stage, however, significant crack parallel tensile stress develops. Energetically, this transition was observed as a reduction in resistance in the R-curve. Specifically, the onset of R-curve reduction occurs at approximately $\Delta a = 40$ mm for the 2.4 mm tab, where the fracture surface transition begins.

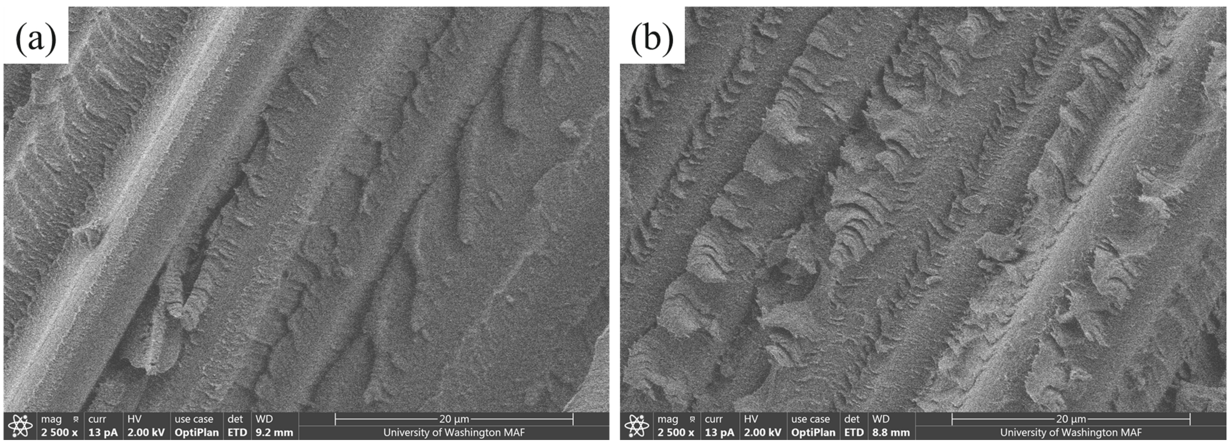

Figure 6: SEM fractography of HOI specimens: (a) region near the initial crack tip under low crack parallel tensile stress; (b) region near final failure under high crack parallel tensile stress.

4 Conclusions

Classical LEFM and idealized line-crack models generally assume that crack parallel stress has negligible influence on fracture behavior. Motivated by recent gap test studies demonstrating stress-state dependence of fracture energy and FPZ size, the present study investigated the effect of crack parallel tensile stress on interlaminar fracture in carbon fiber composites through a newly developed Half Open-I (HOI) test. The HOI configuration enables direct evaluation of crack parallel tensile stress effects without requiring specialized fixtures or complex specimen geometries. The measured R-curve initially agrees with conventional DCB fracture resistance values, but begins to decrease once the crack parallel tensile stress exceeds approximately 50% of the UD tensile strength. This behavior suggests that quasibrittle effects become increasingly significant under high crack parallel tensile stress, resulting in a reduction in interlaminar crack growth resistance that cannot be fully described by conventional line-crack models. SEM observations further support this interpretation. At elevated crack parallel tensile stress levels, the fracture surface exhibits extensive fiber–matrix separation and microscale resin tearing, indicating a change in the dominant energy dissipation mechanisms during fracture. These results demonstrate that crack parallel tensile stress plays a significant role in the interlaminar fracture of quasibrittle composites. Owing to its simplicity and ability to isolate this effect, the HOI test provides a practical framework for investigating stress-state-dependent fracture behavior and may contribute to the development of more reliable fracture databases and structural life-assessment methodologies for composite materials.

Acknowledgements

This work was supported by ES3 Inc under the AFRL–funded Multitude of Attritable CompoSite Structures (MASS) program. Dr. Salviato also wishes to acknowledge the kind support to this work provided by the

Rao and Usha Varanasi Endowed Professorship. The authors gratefully acknowledge the support provided by the University of Washington Advanced Composites Center for supplying laboratory space, vacuum facilities, and prepreg composite materials utilized throughout this study. Composite laminate autoclave curing were carried out using the facilities of the Composites Shop, Department of Mechanical Engineering, University of Washington. SEM observations were conducted at the Molecular Analysis Facility, University of Washington. Mechanical testing was performed at the Mechanical Test Laboratory, Department of Mechanical Engineering, University of Washington. The authors sincerely thank the laboratories and institutes, and all the technical staff members of these facilities for their continuous technical assistance, equipment support, and valuable advice throughout specimen fabrication, testing.

References

[1] Rana, S. and Fangueiro, R. Advanced composites in aerospace engineering. In *Advanced Composite Materials for Aerospace Engineering*, pages 1–15. Woodhead Publishing, 2016.

[2] Dimitris I. Chortis. Structural analysis of composite wind turbine blades. 2013.

[3] Elmarakbi, Ahmed. *Advanced Composite Materials for Automotive Applications: Structural Integrity and Crashworthiness*. John Wiley & Sons, 2013.

[4] Ceccato, Chiara and Salviato, Marco and Pellegrino, Carlo and Cusatis, Gianluca. Simulation of concrete failure and fiber reinforced polymer fracture in confined columns with different cross sectional shape. *International Journal of Solids and Structures*, 108:216–229, 2017.

[5] Jeremy Brockmann and Marco Salviato. The Gap test – Effects of crack parallel compression on fracture in carbon fiber composites. *Composites Part A: Applied Science and Manufacturing*, 164:107252, 2023.

[6] Giurgiutiu, Victor. *Stress, Vibration, and Wave Analysis in Aerospace Composites: SHM and NDE Applications*. Academic Press, 2022.

[7] Salviato, Marco and Kirane, Kedar and Ashari, Shiva Esna and Bažant, Zdeněk P and Cusatis, Gianluca. Experimental and numerical investigation of intra-laminar energy dissipation and size effect in two-dimensional textile composites. *Composites Science and Technology*, 135:67–75, 2016.

[8] Salviato, Marco and Kirane, Kedar and Bažant, Zdeněk P and Cusatis, Gianluca. Mode I and II interlaminar fracture in laminated composites: a size effect study. *Journal of Applied Mechanics*, 86(9):091008, 2019.

[9] Han-Gyu Kim, Ryan Howe, Richard Wiebe, S Michael Spottswood, Patrick J O'Hara, and Marco Salviato. Experimental characterization of cohesive laws for mode-II interlaminar fracture in geometrically scaled composites using through-thickness deformation analysis. *Engineering Fracture Mechanics*, 326:111361, 2025.

[10] Sota Oshima, Marco Salviato, Keita Ushijima, and Naoki Sugiura. Effect of matrix resin types on R-curves and microscopic failure processes during transverse cracking in CFRP laminates. *Composite Structures*, page 119543, 2025.

[11] Hojo, Masaki and Ando, Tadashi and Tanaka, Mototsugu and Adachi, Taiji and Ochiai, Shojiro and Endo, Yoshihiro. Modes I and II interlaminar fracture toughness and fatigue delamination of CF/epoxy laminates with self-same epoxy interleaf. *International Journal of Fatigue*, 28(10):1154–1165, 2006.

[12] Paul, D and Kelly, L and Venkayya, V and Hess, Thomas. Evolution of US military aircraft structures technology. *Journal of Aircraft*, 39(1):18–29, 2002.

[13] Frey, C. and Dölling, S. and Becker, W. Closed-form analysis of interlaminar crack initiation in angle-ply laminates. *Composite Structures*, 257:113060, 2021.

[14] Zdeněk P. Bažant, Jia-Liang Le, and Marco Salviato. *Quasibrittle fracture mechanics and size effect: A first course*. Oxford University Press, 2021.

[15] Salviato, Marco and Phenisee, Sean and Deleo, Antonio and Pelessone, Daniele and Flores, Mark. A novel discrete, mesoscale modeling framework for the simulation of the damaging and fracturing behavior of composites. In *ASME international mechanical engineering congress and exposition*, volume 86717, page V009T12A015. American Society of Mechanical Engineers, 2022.

[16] Marco Salviato, Sean E. Phenisee, Antonio A. Deleo, Daniele Pelessone, and Mark Flores. To the mesoscale and beyond! Capturing complex damage mechanisms in composites via simple, physics-based, discrete mathematical models of fibers and matrix. In *Proceedings of the American Society for Composites-thirty-eighth technical conference*, 2023.

[17] Bažant, Zdeněk P. and Planas, J. *Fracture and Size Effect in Concrete and Other Quasibrittle Materials*. CRC Press, 1998.

[18] Nguyen, Hoang and Pathirage, Madura and Rezaei, Masoud and Issa, Mohsen and Cusatis, Gianluca and Bažant, Zdeněk P. New perspective of fracture mechanics inspired by gap test with crack-parallel compression. *Proceedings of the National Academy of Sciences*, 117(25):14015–14020, 2020.

[19] Lyu, Yuhui and Pathirage, Madura and Nguyen, Hoang T and Bažant, Zdeněk P and Cusatis, Gianluca. Dissipation mechanisms of crack-parallel stress effects on fracture process zone in concrete. *Journal of the Mechanics and Physics of Solids*, 181:105439, 2023.

[20] Tschegg, E. K. and Elser, M. and Stanzl-Tschegg, S. E. Biaxial Fracture Tests on Concrete—Development and Experience. *Cement and Concrete Composites*, 17(1):57–75, 1995.

[21] Li, Linfei and Wang, Boning and Xu, Houlin and Nguyen, Hoang T and Bažant, Zdeněk P and Hubler, Mija H. Crack-parallel stress effect on fracture of fiber-reinforced concrete revealed by gap tests. *Journal of Engineering Mechanics*, 150(4):04024011, 2024.

[22] Kassapoglou, Christos. *Design and Analysis of Composite Structures: With Applications to Aerospace Structures*. John Wiley & Sons, 2013.

[23] Baker, Alan and Dutton, Stuart and Kelly, Donald. *Composite Materials for Aircraft Structures*. AIAA Education Series. American Institute of Aeronautics and Astronautics, Reston, VA, 2nd edition, 2004.

[24] Wang, John T. Continuum Damage Mechanics Based Explicit 3D Progressive Failure Analysis of Composite Laminates. In *The Aircraft Airworthiness and Sustainment Conference*, 2015. NF1676L-21070.

[25] Tsai, Stephen W. and Melo, José Daniel D. *Composite Materials Design and Testing: Unlocking Mystery with Invariants*. Composites Design Group Stanford, UK, 2015.

[26] Clay, Stephen B. and Knoth, Philip M. Experimental results of quasi-static testing for calibration and validation of composite progressive damage analysis methods. *Journal of Composite Materials*, 51(10):1333–1353, 2017.

[27] Syensqo. CYCOM® 977-3 – 350°F (177°C) curing toughened epoxy resin. `https://www.syensqo.com/en/product/cycom-977-3`, 2025. Accessed: 2025-07-10.

[28] University of Washington Advanced Composites Center. Advanced Composites Center. `https://www.uwacc.uw.edu/`, 2026. Visited on 05/29/2026.

[29] ASTM International. Standard Test Method for Mode I Interlaminar Fracture Toughness of Unidirectional Fiber-Reinforced Polymer Matrix Composites. ASTM D5528/D5528M–21, 2021. West Conshohocken, PA. DOI: 10.1520/D5528_D5528M-21.

[30] Chen, Jiacheng. Comprehensive Investigation of Quasibrittle Fracture of IM7/977-3 Laminates via Size Effect Analysis. Master's thesis, University of Washington, 2023.

[31] Murri, Gretchen B. Effect of Data Reduction and Fiber-Bridging on Mode I Delamination Characterization of Unidirectional Composites. In *Proceedings of the 26th ASC Annual Technical Conference*, number NF1676L-12684, Montreal, Quebec, Canada, September 2011. NASA Conference Paper, Document ID: 20110015832.

[32] Gretchen B. Murri. Evaluation of Delamination Onset and Growth Characterization Methods Under Mode I Fatigue Loading. Technical report, 2013.

[33] University of Washington. Molecular Analysis Facility. `https://maf.uw.edu/`, 2025. Accessed: 2026-02-24.

[34] University of Washington Molecular Analysis Facility. APREO-S Variable Pressure Scanning Electron Microscope. `https://www.moles.washington.edu/maf_tools/apreo-variable-pressure-sem/`, 2026. Accessed: 2026-02-24.